Bioorganic & Medicinal Chemistry Letters xxx (2015) xxx–xxx

Contents lists available at ScienceDirect

Bioorganic & Medicinal Chemistry Letters

journal homepage: www.elsevier.com/locate/bmcl

Synthesis and multiparametric evaluation of thiadiazoles and oxadiazoles as diacylglycerol acyltransferase type 1 inhibitors

Patrick Mougenot [a,*], Claudie Namane [a], Eykmar Fett [a], Florence Goumy [a], Rommel Dadji-Faïhun [a], Gwladys Langot [a], Catherine Monseau [a], Bénédicte Onofri [a], François Pacquet [a], Cécile Pascal [b], Olivier Crespin [a], Majdi Ben-Hassine [a], Jean-Luc Ragot [a], Thao Van-Pham [a], Christophe Philippo [a], Florence Chatelain-Egger [a], Philippe Péron [a], Jean-Christophe Le Bail [a], Etienne Guillot [a], Philippe Chamiot-Clerc [a], Marie-Aude Chabanaud [a], Marie-Pierre Pruniaux [a], Jérôme Ménegotto [c], Friedemann Schmidt [d], Olivier Venier [a], Fabrice Viviani [e,†], Eric Nicolai [a,*]

[a] Sanofi-aventis R&D, 91385 Chilly-Mazarin, France
[b] Sanofi-aventis R&D, 69280 Marcy-l'Etoile, France
[c] Evotec, 31036 Toulouse, France
[d] Sanofi-aventis Deutschland GmbH, Industriepark Hoechst, 65926 Frankfurt am Main, Germany
[e] GlaxoSmithKline, 91951 Les Ulis, France

ARTICLE INFO

Article history:
Received 2 October 2015
Revised 10 November 2015
Accepted 14 November 2015
Available online xxxx

Keywords:
Diacylglycerol acyltransferase type 1
DGAT-1 inhibitors
Thiadiazole
Oxadiazole
Solubility
Metabolic lability

ABSTRACT

Chemical modulation of a formerly disclosed DGAT-1 inhibitor resulted in the identification of a compound with a suitable profile for preclinical development. Optimisation of solubility is discussed and a PK/PD study is presented.

DGATs (diacylglycerol acyltransferases) are enzymes which catalyse the final step of the major pathway of triglyceride synthesis. DGAT-1[1] and DGAT-2[2] are encoded by two different genes and are expressed in tissues associated with triglyceride metabolism, particularly in adipose tissue, liver, mammary glands, small intestine and muscle.[1,2] DGAT-1 is anchored in ER membrane and contains approximately 500 very hydrophobic amino acid residues.

Since 2007, several small molecules[3] have entered clinical trials as DGAT-1 inhibitors. Presently, two of them are still in clinical development; pradigastat (Fig. 1) is in phase III since 2012 for familial hypertriglyceridemia[4] and P-7435 is in phase I for obesity.[5]

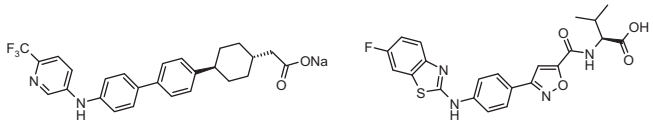

Figure 1. Pradigastat and P-7435.

In 2012, we disclosed new and potent thiadiazoles as DGAT-1 inhibitors[6] (Fig. 2), which completely blocked TG production in vivo after an acute lipid challenge. Unfortunately, the low solubility of these compounds prevented further pharmacological studies as no acceptable vehicle compatible with metabolic readouts could be identified[7] (see Table 1).

Abbreviations: DBU, 1,8-diazabicyclo[5.4.0]undec-7-ene; DCM, dichloromethane; DIAD, diisopropylazodicarboxylate; DMF, dimethylformamide; CDI, carbonyldiimidazole; met. lia., metabolic liability; MC, methylcellulose; ND, not determined; PK, pharmacokinetic; PyBroP, bromotrispyrrolidinophosphonium hexafluorophosphonate; sol., solubility; T, tween; TEA, triethylamine; TFA, trifluoroacetic acid; TG, triglycerides; THF, tetrahydrofuran.

* Corresponding authors.
† Present address.

http://dx.doi.org/10.1016/j.bmcl.2015.11.046
0960-894X/

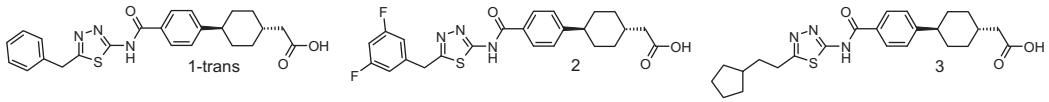

Figure 2. Compounds from Ref. 6.

Table 1
Lead compounds **1**-*trans*, **2**, and **3**

Compd	Enz. DGAT-1 IC_{50} (μM)[8]	Cell. DGAT-1 IC_{50} (μM)[9]	% met. h/m/r[10]	Caco2 (10^{-7} cm/s)[11]	Sol. pH = 7.4 (μM)[12]
1-*trans*	0.036	0.029	0:5:11	112	<2
2	0.009	0.048	1:7:1	135	<2
3	0.019	0.012	36:5:10	90	<2

It should be noted that the internal Sanofi solubility standard for preclinical candidate selection is set to 100 μM in phosphate buffer at pH = 7.4 or in water.

Since compound **3** was the most potent cellular inhibitor in this series but suffered from low solubility in phosphate buffer at pH 7.4 and moderate metabolic stability in human microsomes, we decided to take it as a model compound to address both the solubility and metabolic stability issues by introduction of polarity at appropriate sites.

The metabolic lability of **3** is due to phase I oxidative metabolism with a 63% contribution of cytochrome CYP3A4. Such liability can be addressed by in silico models derived from 3D structure/

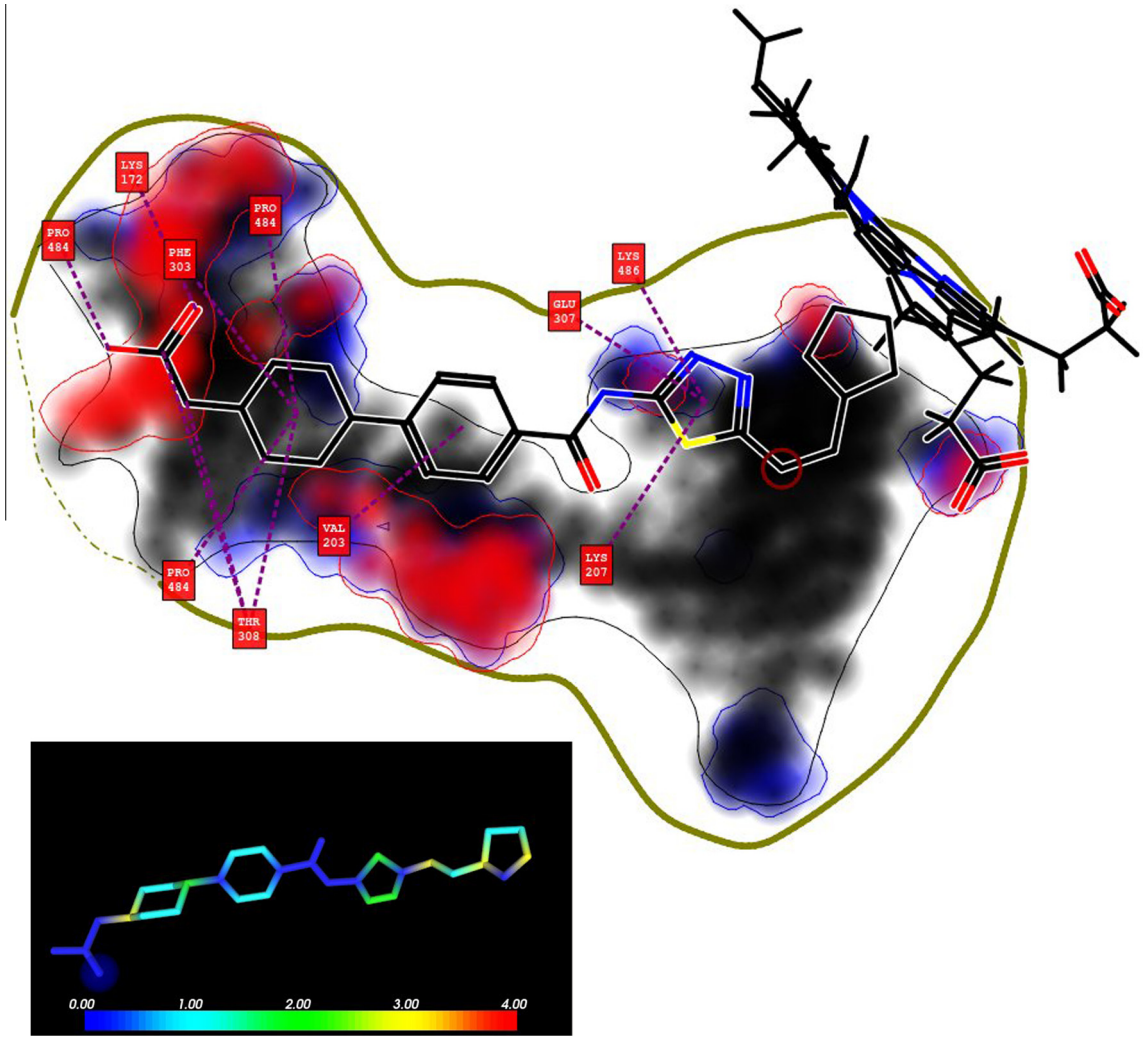

Figure 3. Prediction of sites of metabolism (SOM) with Metasite 5.0, based on Astex CYP3A4 + ketoconazole with reactivity correction for compound **3**. Likelihood of metabolism is indicated in a heatmap representation (small insert). The primary SOM is predicted at the benzylic position of the thiadiazole scaffold (marked as red circle). Black fields indicate hydrophobic ligand recognition by the cytochrome complex, red fields indicate hydrogen bond acceptor recognition, such as oxygen, and blue fields represent hydrogen bond donor recognition. Introduction of polarity into a hydrophobic region or introduction of opposite polarity is suggestive for a decrease in the molecular recognition, potentially leading to a decrease in the rate of metabolism.[14]

Please cite this article in press as: Mougenot, P.; et al. *Bioorg. Med. Chem. Lett.* (2015), http://dx.doi.org/10.1016/j.bmcl.2015.11.046

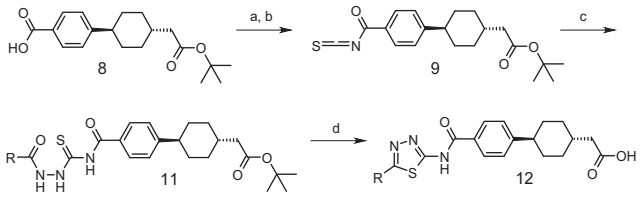

Scheme 1. Synthesis of compound **12**. Reagents and conditions: (a) $(COCl)_2$, DCM, (b) KSCN, CH_3CN; (c) $RCONHNH_2$ **10**, CH_3CN, reflux; (d) TFA, four steps 30–65%.

ligand based methods. Identification of the causal metabolic 'hot spots' in compound **3** would allow the design of improved candidates. We first applied the MetaSite[13] prediction tool that includes 3D models of the most important human cytochromes, including CYP3A4, and allows recognition of labile sites of metabolism (SOM). Since CYP3A4 was the main contributor to its metabolism we assessed compound **3** in a CYP3A4 model from a ketoconazole co-crystal, with built-in corrections for reactivity of the enzyme and ligand. The predicted primary sites of metabolism were located on the cyclopentylethyl fragment (Fig. 3).

In accordance with MetaSite predictions, we introduced oxygen atoms at different positions of the cyclopentylethyl moiety to block oxidative metabolism and to assess the effect on solubility in parallel.

The synthesis[15] of corresponding compounds **12a–c** is depicted in Scheme 1 starting from the carboxylic acid **8**. The successive reactions with oxalyl chloride and potassium isothiocyanate gave the acylisothiocyanate **9**. Addition of the hydrazide **10** followed by trifluoroacetic acid treatment gave the thiadiazole **12**.

As shown in Table 2, the introduction of an ether function on the cyclopentylethyl group led to an increase in metabolic stability and solubility but also to a drop in activity compared to compound **3**. Compounds **12b** and **12c** displayed acceptable solubility up to 90 μM at pH = 7.4 but at the expense of potency. On the other hand, compound **12a** retained good potency but its solubility was too low.

Encouraged by the favourable effect on solubility obtained with compounds **12a–c**, we considered a more aggressive strategy to address this issue: (i) introduction of heteroatoms at other sites of the scaffold; (ii) thiadiazole replacement by more soluble five-membered heterocycles; (iii) introduction of solubilising groups and (iv) salt formation (Fig. 4).

As had been shown earlier,[6] the aliphatic acid appears to be essential for maintaining the enzymatic activity. Therefore, we first envisaged the introduction of an oxygen atom between the phenyl and the cyclohexyl moieties whilst keeping the distance between the thiadiazole and the carboxylic acid constant as in compounds **4**-*cis*/*trans* and **5**-*cis*/*trans*.

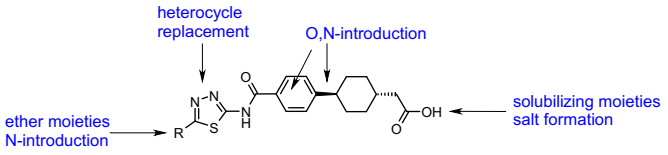

Figure 4. Strategy to increase solubility of the thiadiazole series.

The synthesis[15] of compounds **4**-*cis* and **5**-*cis* is depicted in Scheme 2 starting from the carboxylic acid **6** which is transformed into the acid chloride with oxalyl chloride. Subsequent coupling reactions with 2-amino-1,3,4-thiadiazoles led to the amides **7**. We also used PyBroP® for the synthesis of amides **7** from carboxylic acid **6** and 2-amino-[1,3,4]thiadiazoles. Finally, the corresponding carboxylic acids **4**-*cis* and **5**-*cis* were obtained after basic hydrolysis.

As seen in Table 3, *cis* derivatives were at least ten fold more potent that their *trans* counterparts which could be explained by a better alignment when superimposed on **1**-*trans* as shown in Figure 5.

Unfortunately, the aqueous solubility at pH = 7.4 of compounds **4**-*cis* and **5**-*cis* was not dramatically improved compared to **1**-*trans* and **2**. On the other hand, these ether analogues were found to be very potent in enzymatic and cell-based assays. Overall, compound **5**-*cis* displayed a favourable profile with very good potency, good metabolic stability and intestinal permeability but only a limited gain in solubility, which made it a good candidate for salt screening.

In order to assess a possible synergistic effect between the incremental improvements in solubility seen in **12a** and **5**-*cis*, we introduced a second oxygen in compound **12a**, in the hope of further improving solubility. The synthesis[15] of compound **16** is depicted in Scheme 3 starting from the carboxylic acid **6**. The successive reactions with oxalyl chloride and potassium isothiocyanate gave the benzoylisothiocyanate **13**. Addition of cyclopentyloxymethylhydrazide followed by trifluoroacetic acid treatment gave the thiadiazole **15**. Finally, basic hydrolysis led to the carboxylic acid **16** (see Table 4).

As expected, solubility of compound **16** was improved compared to **12a** and **5**-*cis* but still remained too low.

Due to the insufficient improvement in solubility by the introduction of oxygen atoms in the above compounds, we decided to assess the effect of nitrogen insertion.

We first tried the replacement of the phenyl by a pyridyl in compound **4**-*cis*. The general synthesis[15] is depicted in Scheme 4. Starting from the ethyl hydroxynicotinic ester **19** and *cis*-*tert*-butyl 4-hydroxycyclohexanecarboxylic ester **20** in a Mitsunobu reaction gave, after hydrolysis, the carboxylic acid **22**. The subsequent

Table 2
Modulation of cyclopentyl derivatives **3**, **12a–c**

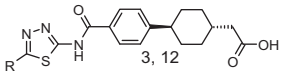

Compd	R	Enz. DGAT-1 IC_{50} (μM)	Cell. DGAT-1 IC_{50} (μM)	% met. h/m/r	Caco2 (10^{-7} cm/s)	Sol. pH = 7.4 (μM)
3	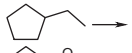	0.019	0.012	36:5:10	90	<2
12a	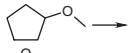	0.038	0.066	3:0:0	103	9
12b	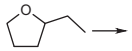	0.144	ND	9:8:3	72	90
12c	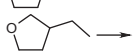	0.233	ND	ND	ND	95

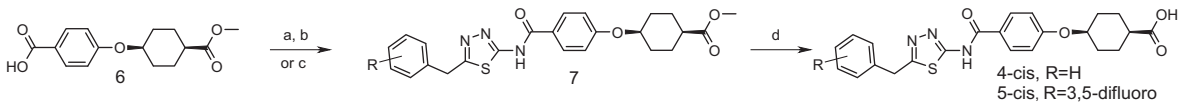

Scheme 2. Synthesis of compounds **4**–**5**. Reagents and conditions: (a) $(COCl)_2$, DCM; (b) 5-(3,5-difluorobenzyl)-2-amino[1,3,4]thiadiazole, pyridine, CH_3CN (2 steps, 86%); (c) 5-benzyl-2-amino-[1,3,4]thiadiazole, PyBroP®, 26%; (d) $LiOH{\cdot}H_2O$, THF, H_2O, 56–78%.

Table 3
Compounds **4**-*cis* and **5**-*cis*

Compd	Enz. DGAT-1 IC_{50} (μM)	Cell. DGAT-1 IC_{50} (μM)	% met. h/m/r	Caco2 (10^{-7} cm/s)	Sol. pH = 7.4 (μM)
4-*cis*	0.016	0.028	3:27:22	15	2
4-*trans*	0.280	ND	ND	ND	ND
5-*cis*	0.011	0.013	1:42:9	29	4
5-*trans*	0.160	0.076	1:9:8	30	ND

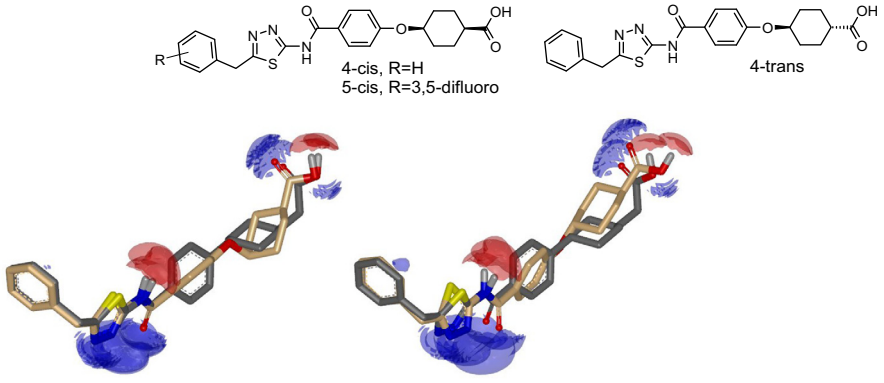

Figure 5. Compounds **4**-*cis* and **4**-*trans*. Left: The alignment[16] of **4**-*cis* with **1**-*trans* (shown in grey) suggests a very good match of the cyclohexyl ring moiety, while the electrostatic fields of the carboxylates strongly overlap. Right: the configuration of **4**-*trans* leads to a deviation of the carboxylate electrostatic fields, with less overlap with **1**-*trans*.

coupling reaction with 2-amino-1,3,4-thiadiazoles led to the amides **23**. Finally, treatment with trifluoroacetic acid provided compound **24**.

As shown in Table 5, compound **24a** displayed a significant enhancement of solubility at pH = 7.4, but associated with a drop in Caco2 permeability. Introduction of the chlorine substituent led to compound **24b** with an improvement of Caco2 permeability but, unfortunately, lower solubility.

On the other hand, the introduction of a nitrogen atom close to the thiadiazole ring gave the diaminothiadiazoles **25**, synthesized according to Scheme 2. Compound **25a** showed a slight enhancement of solubility at pH = 1 and pH = 7.4. Replacement of the western cyclopentyl by a phenyl moiety led to diaminothiadiazole **25b**, a potent compound with a low solubility. Both compounds had low Caco2 permeability (see Table 6).

In view of the limited improvement in solubility through the introduction of heteroatoms, we tried to change the thiadiazole core to a more polar five-membered ring such as an oxadiazole.[17] We synthesized the 1,3,4- and the two 1,2,4-oxadiazole regioisomers[18] in the phenylcyclohexyl and phenoxycyclohexyl series to explore their solubility according to Scheme 5 below.

Treatment of benzoyl chloride with sodium cyanamide followed by hydroxylamine yielded 3-amino-1,2,4-oxadiazole **27**. Coupling with the carboxylic acid **8** and trifluoroacetic acid deprotection led to compound **28**.

Treatment of benzyl cyanide with hydroxylamine followed by trichloroacetyl chloride led to the 5-trichloromethyl-1,2,4-oxadiazole **30**. Nucleophilic substitution with the carboxamide **31** in the presence of NaH and hydrolysis led to the expected compound **32**.

The 1,3,4-oxadiazole **28b** showed a dramatic increase in solubility at pH = 7.4, but a significant decrease in potency compared to the thiadiazole **28a**. The 1,2,4-oxadiazole regioisomers **28c** and **28d** showed a significant increase in solubility at pH = 7.4 compared to the thiadiazole **1**-*trans* but a loss in potency. Finally, in the phenoxycyclohexyl series, compounds **32a**–**b** showed a very high solubility, well above our internal standard for clinical candidates, but their low metabolic stability in rodents prevented us from selecting them for further in vivo studies (see Table 7).

In the absence of a co-crystal structure for DGAT-1, we turned for further guidance to the ligand-based alignment of **4**-*cis* with a substrate of DGAT-1, namely coenzyme A. The latter has been described as a competitive substrate for a synthetic ligand.[19] This finding led us to hypothesise a potential overlap of the ligand binding sites, and to closely examine shared hydrophilic and hydrophobic sites. Several cocrystal structures of acyltransferases have been published so far, disclosing various coenzyme A fatty acid esters in their bioactive conformation.[20] Interestingly, many of these substrates share an elongated bend structure of the peptidic moiety. We tested alignments of **4**-*cis* with decanoyl-coenzyme A in bioactive conformation (see Fig. 6). Both compounds apparently share key pharmacophore recognition features. The carboxylic acid of **4**-*cis* is linked to the proximal phosphate ester, the cyclohexyl moiety of **4**-*cis* to the geminal dimethyl group of coenzyme A, while the arylamide of **4**-*cis* is matched to the aliphatic amide and the thiadiazole core of **4**-*cis* to the cleavable thioester of the substrate. The distal benzyl moiety of **4**-*cis* is matched to the fatty acid chain, supporting the introduction of aromatic or aliphatic hydrophobic substituents. If this binding mode is valid, the introduction of polar

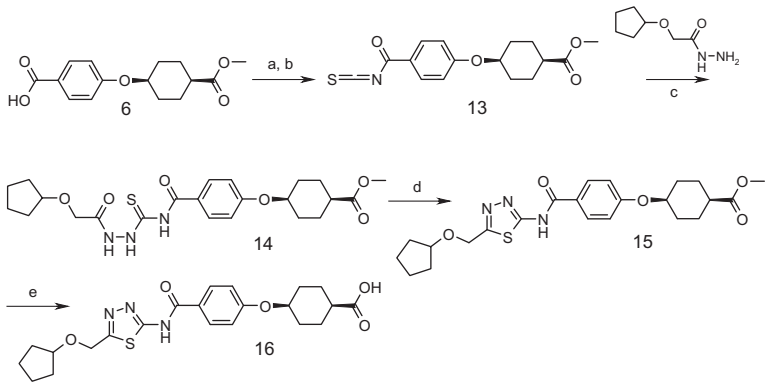

Scheme 3. Synthesis of compound **16**. Reagents and conditions: (a) $(COCl)_2$, DCM, (b) KSCN, CH_3CN, (c) CH_3CN, reflux, 89%, three steps, (d) TFA, (e) $LiOH{\cdot}H_2O$, THF, H_2O, 87%, two steps.

Table 4
Compound **16**

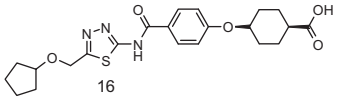

Compd	Enz. DGAT-1 IC_{50} (μM)	Cell. DGAT-1 IC_{50} (μM)	% met. h/m/r	Caco2 (10^{-7} cm/s)	Sol. pH = 7.4 (μM)
16	0.012	0.017	5:8:1	41	18

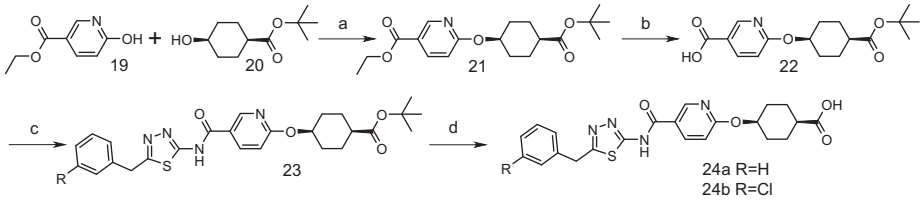

Scheme 4. Synthesis of compound **24**. Reagents and conditions: (a) DIAD, Ph_3P, 47%; (b) $LiOH{\cdot}H_2O$, THF, methanol, 98%; (c) 5-(3-benzyl)-[1,3,4]thiadiazol-2-ylamine (or chloro derivative), PyBroP®, DIEA, 63% (49%); (d) TFA, DCM, 80% (90%).

Table 5
Modulation of the R moiety in pyridines **24**

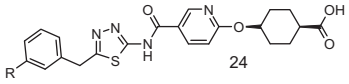

Compd	R	Enz. DGAT-1 IC_{50} (μM)	Cell. DGAT-1 IC_{50} (μM)	% met. h/m/r	Caco2 (10^{-7} cm/s)	Sol. pH = 7.4 (μM)
24a	H	0.045	0.135	1:23:37	11	89
24b	Cl	0.055	0.085	2:56:27	17	8

and solubilising groups is to be envisioned only at the eastern part of the molecule towards the phosphate of coenzyme-A.

This prompted us to try to address the solubility issue with the preparation of amide derivatives of **1**-*trans* bearing solubilising moieties.[21]

Scheme 6 depicts the synthesis of compounds **33**[15] obtained from the corresponding carboxylic acid **1**-*trans* with a panel of amines in the presence of PyBroP®.

As shown in Table 8, the carboxamide compound **33a** retained the capacity to inhibit DGAT-1 but did not display improved solubility. Further elongation gave compounds **33b–f**. Replacement of the primary amide with hydroxydimethylethyl, dihydroxypropyl or methoxyethyl amide derivatives led to less active compounds **33b–d** without any improvement in solubility. Morpholino or dimethylamino derivatives **33e** and **33f** showed slight but not significant enhancement of solubility only at pH = 1.

Therefore, although heteroatom introduction and/or thiadiazole replacement by 1,2,4-oxadiazole lead us to identify several compounds with dramatic improvements in solubility (**12b**, **12c**, **24a**, **28b**, **28c**, **32a** and **32b**) unfortunately none of these compounds displayed an optimal overall profile suitable for clinical candidate nomination.

Table 6
Modulation in aminothiadiazoles **25**

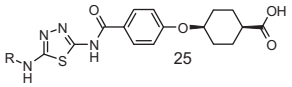

Compd	R	Enz. DGAT-1 IC_{50} (μM)	Cell. DGAT-1 IC_{50} (μM)	% met. h/m/r	Caco2 (10^{-7} cm/s)	Sol. pH = 1 (μM)	Sol. pH = 7.4 (μM)
25a		0.022	0.009	2:3:4	6	12	26
25b		0.004	0.003	11:8:4	6	<2	<2

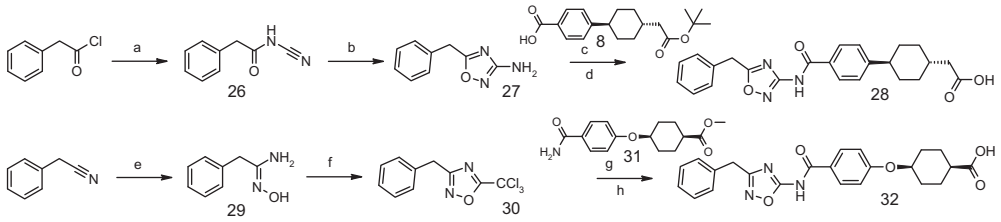

Scheme 5. Synthesis of compounds **28c–d** and **32a–b**. Reagents and conditions: (a) NaNHCN, THF, reflux. (b) $HONH_2$·HCl, pyridine, 53%, two steps. (c) Compound **8**, CDI, DBU, DMF, 100 °C, 12%. (d) TFA, DCM, 25%. (e) $HONH_2$·HCl, TEA, ethanol, reflux, 49%. (f) Cl_3CCOCl, pyridine, toluene, 85 °C, 90%. (g) Compound **31**, NaH, THF, 45%. (h) LiOH·H_2O, THF, water, 51%.

Table 7
Five-membered ring modulation

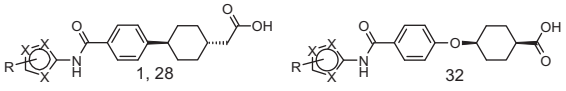

Compd		Enz. DGAT-1 IC_{50} (μM)	Cell. DGAT-1 IC_{50} (μM)	% met. h/m/r	Caco2 (10^{-7} cm/s)	Sol. pH = 1 (μM)	Sol. pH = 7.4 (μM)
1-*trans*	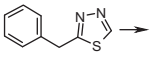	0.036	0.029	0:5:11	112	<2	<2
28a	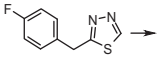	0.600	0.130	ND	ND	<2	<2
28b	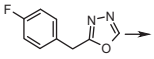	1.39	ND	ND	ND	<2	446
28c	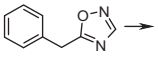	0.286	ND	ND	ND	<2	129
28d	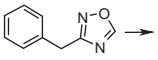	0.253	ND	ND	ND	<2	41
32a	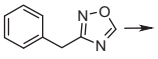	0.057	ND	2:100:53	29	<2	274
32b	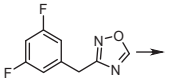	0.120	0.310	1:99:61	9	<2	813

Finally, to combine optimal activity/e-ADMET profile with a solubility level appropriate for further development, we used compounds **1**-*trans* and **5**-*cis* to perform a salt screening with a panel of pharmaceutically acceptable bases.[22]

Four salts (sodium, potassium, calcium and arginine) were identified and confirmed in crystalline form for compound **1**-*trans*. The sodium and arginine salts were scaled-up and analysed by differential scanning calorimetry (DSC) and thermal gravimetric analysis (TGA). Both salts showed loss of weight or structural modifications before the melting point which made them unsuitable for further development.

Compound **5**-*cis* led to seven salts confirmed in crystalline form; sodium, potassium, calcium, *N*-methyl glucamine, lysine, arginine, trometamol, and choline. The potassium salt was abandoned due to synthesis reproducibility issues. The arginine, trometamol, lysine, and sodium salts were scaled-up and analysed by DSC and TGA.[23] Salting out was observed in water with the sodium salt. The arginine and trometamol salts were polymorphic. Only the lysine salt displayed an acceptable profile for further development.

The lysine salt of compounds **5**-*cis*, **5**-*cis*L,[24] showed a large increase in aqueous solubility compared to the carboxylic acid

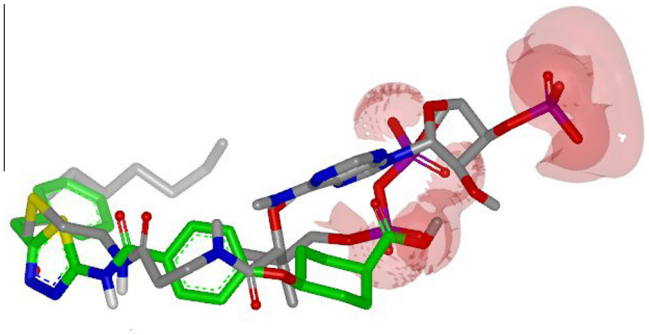

Figure 6. Ligand-based alignment for compound **4**-*cis* (shown in green) and decanoyl-coenzyme A in a bioactive conformation (pdb code 4MFK). Negative charge is represented by red shaded fields, and overlaps to a great extent between the carboxylic acid of the ligand and the proximal phosphoric acid ester of decanoyl-coenzyme A.

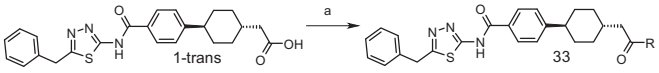

Scheme 6. Synthesis of compounds **34a–f**. Reagents and conditions: (a) PyBroP®, triethylamine, amines, DMF, 7–68%.

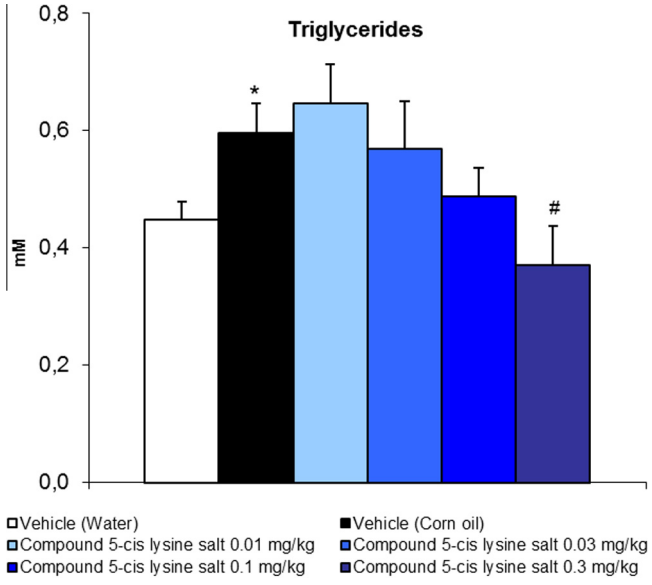

Figure 7. Lipid challenge assay with compound **5**-*cis*L.

Table 8
Modulation of R moiety in amides **34a–f**

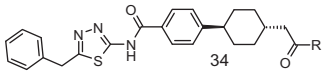

Compd	R	Enz. DGAT-1 IC_{50} (μM)	Sol. pH = 1 (μM)	Sol. pH = 7.4 (μM)
1-*trans*	← OH	0.036	<2	<2
33a	← NH_2	0.048	<2	<2
33b	← HN, OH	0.092	<2	<2
33c	← NH, OH, OH	0.081	<2	<2
33d	← NH, O	0.088	<2	<2
33e	← NH, N, O	0.122	7	<2
33f	← NH, N	0.279	6	<2

Table 9
Comparison between carboxylic acid form and lysine salt of compound **5**-*cis*

Compd	Sol. water (μM)	Sol. pH = 7.4 (μM)	Bioavailability in % (in rats)
5-*cis*	<21	4	4
5-*cis*L	864*	8	40

* pH measured = 9.0.

Table 10
Pharmacokinetic and distribution profile for compound **5**-*cis*L in rats after a single oral administration (10 mg/kg in MC/T)

Distribution C_{max} (ng/ml/μM)				
Plasma	Liver	Small intestine	Heart	Brain
6440/13.2	121,000/247.9	6980/14.3	2040/4.2	75.8/0.16

Plasma half life: 7.4 h; T_{max}: 4 h.

form. To confirm the interest of this lysine salt form, we performed a head to head bioavailability comparison in rats with the free carboxylic acid and found a very significant improvement (40% compared to 4%) in the bioavailability of the lysine salt form (see Table 9).

Compound **5**-*cis*L showed a good pharmacokinetic profile with a maximal plasma concentration (C_{max}) of 13.2 μM and a half-life of 7.4 h, both compatible with pharmacological studies. It also showed a large tissue distribution associated with a concentration of 14.3 μM in the small intestine, the target tissue for the lipid challenge test (see Table 10).

As shown in Figure 7 and 5-*cis*L, administered at 0.01, 0.03, 0.1, and 0.3 mg/kg, significantly and dose-dependently decreased plasma TG (ED_{50} = 0.08 mg/kg), in an acute lipid challenge test[25] 1 h after oral administration.

In further studies, compound **5**-*cis*L was compared to the free carboxylic acid form in the acute lipid challenge test. Under these conditions **5**-*cis*L given orally at 0.3 mg/kg inhibited the TG rise induced by a corn oil challenge by 153% ($p < 0.05$), whereas the carboxylic acid inhibited the TG rise by only 91% at the same dose. The duration of action was similar for the two compounds with a maximal effect observed between 1 and 3 h after oral administration (−76% at 1 mg/kg at 3 h for the carboxylic acid and −101% at 0.3 mg/kg at 3 h for the lysine salt).

In conclusion, among the different strategies used to improve the solubility of this chemical series, the best results were obtained by thiadiazole replacement leading to the oxadiazole **32a** which unfortunately displayed insufficient metabolic stability in rodents for in vivo evaluation. Finally, a salt screen of best thiadiazole leads **1**-*trans* and **5**-*cis* provided the lysine salt **5**-*cis*L as a potential development candidate displaying good aqueous solubility in water and a favourable PK/PD profile. Evaluation of this compound in an acute lipid challenge test showed a drop in TG at a low administered dose. On the basis of its overall profile, compound **5**-*cis*L was selected for preclinical development and results will be reported elsewhere in due course.

Acknowledgment

The authors would like to thank Fiona Ducrey for guidance and proof reading this Letter.

References and notes

1. (a) Cases, S.; Smith, S.; Zheng, Y.-W.; Myers, H. M.; Lear, R. S.; Sande, E.; Novak, S.; Collins, C.; Welch, C. B.; Lusis, A. J.; Erikson, S. K.; Farese, R. V., Jr. *Proc. Natl. Acad. Sci. U.S.A.* **1998**, *95*, 13018; (b) Sturley, S. L.; Oelkers, P. U.S. Pat. 6,100,077.
2. Cases, S.; Stone, S. J.; Zhou, P.; Yen, E.; Tow, B.; Lardizabal, K. D.; Voelker, T.; Farese, R. V., Jr. *J. Biol. Chem.* **2001**, *276*, 38870.
3. DeVita, R. J.; Pinto, S. *J. Med. Chem.* **2013**, *56*, 9820.
4. Notte, G. T. *Ann. Rep. Med. Chem.* **2013**, *48*, 451.
5. (a) Trialtrove database: P-7435 in Phase I completed with the status discontinued. Consulted in November 2015; (b) Cortellis database: P-7435 in Phase I with the status discontinued. The structure has been disclosed but not in a peer-review source. Consulted in November 2015.
6. Mougenot, P.; Namane, C.; Fett, E.; Camy, F.; Dadji-Faïhun, R.; Langot, G.; Monseau, C.; Onofri, B.; Pacquet, F.; Pascal, C.; Crespin, O.; Ben-Hassine, M.; Ragot, J.-L.; Van-Pham, T.; Philippo, C.; Chatelain-Egger, F.; Péron, P.; Le Bail, J.-C.; Guillot, E.; Chamiot-Clerc, P.; Chabanaud, M.-A.; Pruniaux, M.-P.; Schmidt, F.; Venier, O.; Nicolaï, E.; Viviani, F. *Bioorg. Med. Chem. Lett.* **2012**, *22*, 2497.
7. Zimmermann, S.; Zarse, K.; Schulz, T. J.; Siems, K.; Müller-Kuhrt, L.; Birringer, M.; Ristow, M. *Horm. Metab. Res.* **2008**, *40*, 29.
8. Enzymatic assay: (a) compound activity (0.000038–10 μM, final concentration) was measured in a phase-partition based assay using a recombinant human DGAT-1 enzyme (Kristie, *Anal. Biochem.* **2006**, 358). Briefly, the assay was performed in 96-well Isoplate, in a 50 μl final volume, with 100 mM Hepes, 250 mM sucrose, 150 μM 1,2-di-(*cis*-9-octadecenoyl)-sn-glycerol, 40 μM 3*H*-octanoyl-CoA (1 μCi/ml), 10 mM $MgCl_2$ and 0.25 μg of microsomal proteins from Sf9 insect cells overexpressing human DGAT1. The reaction was initiated by the addition of DGAT1 microsomes and carried out for 60 min at 25 °C, then stopped with 10 μl of acetic acid (3.3% final concentration). After 45 min of further incubation at room temperature, 60 μl of BetaPlate Scint cocktail (Perkin Elmer) were added in order to partition lipids from the aqueous phase. Radioactivity of the upper organic phase was determined using a MicroBeta counter (Perkin Elmer). As confirmation of the screening, IC_{50}s were assessed through dose–response in monoplicate. Each run was validated with a reference compound JT-553 described in litterature[8b,8c] (IC_{50}—28 nM ± 3.1, $n > 100$); (b) Fox, B. M.; Furukawa, N.; Hao, X.; Iio, K.; Inaba, T.; Jackson, S. M.; Kayser, F.; Labelle, M.; Li, K.; Matsui, T.; Mcminn, D. L.; Ogawa, N.; Rubenstein, S. M.; Sagawa, S.; Sugimoto, K.; Suzuki, M.; Tanaka, M.; Ye, G.; Yoshida, A.; Zhang, J. WO2004/047755; (c) Dow, R. L.; Andrews, M.; Aspnes, G. E.; Balan, G.; Gibbs, E. M.; Guzman-Perez, A.; Karki, K.; LaPerle, J. L.; Li, J.-C.; Litchfield, J.; Munchhof, M. J.; Perreault, C.; Patel, L. *Bioorg. Med. Chem. Lett.* **2011**, *21*, 6122.
9. Cellular assay: compound activity was measured in vitro using Chang liver cells. Briefly, the day before the assay, cells were seeded in 24-well plates at 1.8×10^5 cells per well. The cells were starved overnight in a DMEM 4.5 g/L glucose medium supplemented with 2% Oleic Acid–Albumin complex. Thereafter, compounds were dispensed into respective wells and the plates were incubated 30 min at 37 °C, 5% CO_2. Then, the substrate (Glycerol [^{14}C] 0.4 μCi/ml final) was added into each well and the plates were incubated 6 h at 37 °C, 5% CO_2. Incubation medium was removed and the cells were washed twice with PBS. After trypsination, cells were centrifuged for 5 min at 1300×*g* and the supernatant was discarded. Lipids were extracted from cell pellets by adding 400 μl of a methanol/dichloromethane/TFA (50:50:0.1%) solution. The samples were sonicated and filtered (0.45 μm). The samples were analysed by HPLC (Waters 2695 with a SunFire® column C18 3 μm 4.6 × 75 mm), with a mobile phase 5% (H_2O + 0.1% TFA), 70% methanol, 25% dichloromethane with a flow of 1.5 ml/min, coupled to a flow scintillation analyzer (Perkin Elmer radiomatic 625T) to separate and quantify the relative amount of all ^{14}C-acylglycerides formed.
10. Metabolic lability: compound is incubated 20 min with human or mouse hepatic microsomal fraction. Metabolisation (Met.)% result corresponds to disappearance of tested compound at the end of the experiment.
11. Caco2 permeability: (a) Grès, M.-C.; Julian, B.; Bourrié, M.; Meunier, V.; Roques, C.; Berger, M.; Boulenc, X.; Berger, Y.; Fabre, G. *Pharm. Res.* **1998**, *15*, 726; (b) Grandi, D. D.; Press, B. *Curr. Drug Metab.* **2008**, *9*, 893.
12. Solubility: 2 mg of compound is incubated in 1 mL of the media for 20 h with a shaker. The media is then filtered. The solubility was determined with an UPLC system using a Acquity HSS C18 (50 * 2.1 mm; 1.8 μm) column with a mobile phase 2–100% of ACN/TFA 0.035% in H_2O/TFA 0.05% in 3.5 min. Solubility at pH = 1 or pH = 7.4 indicated an HCl 0.1 N solution or a phosphate buffer 50 mM pH 7.4, respectively.
13. Cruciani, G.; Carosati, E.; De Boeck, B.; Ethirajulu, K.; Mackie, C.; Howe, T.; Vianello, R. *J. Med. Chem.* **2005**, *48*, 6970.
14. Baringhaus, K.-H.; Hessler, G.; Matter, H.; Schmidt, F. In *Chemoinformatics for Drug Discovery*; Jürgen Bajorath, Ed.; Wiley, 2013.
15. Fett, E.; Mougenot, P.; Namane, C.; Nicolaï, E.; Philippo, C. WO2010/086551.
16. For generating a high-quality 3D alignment we employed our internal application MARS, which performs a combinatorial analysis of ROCS 3D shape-based alignments. The computational procedure has been reported in a previous publication.[6] The best ranked alignment—as determined by the maximum sum of scores—is being reported.
17. Boström, J.; Hogner, A.; Llinàs, A.; Wellner, E.; Plowright, A. T. *J. Med. Chem.* **2012**, *55*, 1817.
18. Fett, E.; Mougenot, P.; Namane, C.; Nicolaï, E.; Philippo, C. WO2012/011081.
19. Cao, J.; Zhou, Y.; Peng, H.; Huang, X.; Stahler, S.; Suri, V.; Qadri, A.; Gareski, T.; Jones, J.; Hahm, S.; Perreault, M.; McKew, J.; Shi, M.; Xu, X.; Tobin, J. F.; Gimeno, R. E. *J. Biol. Chem.* **2011**, *286*, 41838.
20. The protein data bank PDB: http://www.rcsb.org.
21. Wermuth, C. G. *The Practice of Medicinal Chemistry*, 3rd ed.; Academic Press, 2008. Chapter 38, p 767.
22. Panel of bases: sodium hydroxide, potassium hydroxide, calcium hydroxide, *N*-methylglucamine, L-lysine, L-arginine, trometamol, betaine, ammonia, choline.
23. DSC: TA INSTRUMENTS Q200 under nitrogen at 50 ml/mn flow and a rate of 10 °C/min. TGA: TA INSTRUMENTS: TGA Q500 under nitrogen with a rate of 10 °C/min.
24. Procedure: A solution of L-lysine (0.34 g, 2.32 mmol) in 21 mL of a 4:1 mixture MeOH/water was added to the carboxylic acid **5** (1 g, 2.11 mmol) in tetrahydrofuran (70 mL). The mixture was heated at 80 °C within 2 h. After cooling, the precipitate was filtered, washed successively with EtOH/water and twice with EtOH. After drying in vacuum for 48 h, 0.842 g of a white-off solid was obtained.
25. Male C57Bl/6J mice (22–24 g), previously fed ad libitum with a standard laboratory diet and tap water, are fasted 17 h before the treatment. On the day of experiment, mice are treated orally (10 mL/kg) with vehicle (water) or compound at 0.01, 0.03, 0.1 and 0.3 mg/kg prepared in vehicle (n = 10 mice per group) eighteen to one hour before the lipid challenge. At T0, mice are treated with 5 mL/kg of corn oil or with 5 mL/kg of water. One hour after corn oil treatment, blood collection is performed (retro-orbital sinus puncture) under isoflurane anesthesia for assessment of plasma triglycerides. ED_{50} values are calculated using BioSt@t-Speed-LTS 2.0. Statistical analysis are performed using SAS® V8.2 with the Everstat interface: One-way-Anova followed by a Kruskal Wallis test. The significance level is set to 0.05.